Carving from ray-tracing constraints: IRT-carving

[†]M. Andreetto, [‡]S. Savarese, [†]P. Perona

[†]Dept. Electrical Engineering
California Institute of Technology
Pasadena, CA 91125
marco,perona@caltech.edu

[‡]Beckman Institute
University of Illinois Urbana-Champaign
Urbana, IL 61801
silvio@uiuc.edu

Abstract

We present a new algorithm for improving an available (conservative) estimate of the shape of an object using constraints from ray-tracing. In particular, we exploit incoherences between the lit portions of the object - detected on a set of acquired images - and the shadows that the current estimate casts on itself. Whenever a contradiction is found the current estimate is modified in order to remove the inconsistency. Sufficient conditions for the correctness of the algorithm and a discussion of their validity are provided. Finally, we describe a simple implementation of the method and present some preliminary experimental results from computer simulations.

1. Introduction

Computing the shape of an object using optical devices for data acquisition has been an active research field in computer vision, and many different solutions have been proposed over the years. These solutions often reach a compromise among accuracy of the reconstruction, cost of the acquisition hardware and quantity of human interaction required to obtain the final model.

The most popular solutions are active stereo techniques, such as laser stripe scanners or structured light scanners. However, these techniques often require ad hoc and expensive acquisition hardware. Besides, even when no specific hardware is required (e.g., [1]), these techniques usually produce a set of partial range images that require registration or editing in order to obtain the complete final model.

For very low-budget application, such as e-commerce and virtual exhibition on the web, these solutions are still too expensive. This is particularly true when it is necessary to acquire a large number of objects, with relative high amount of human work. A technique suitable for these applications is shape from silhouettes [2] [3] [4]. In shape from silhouettes an estimate of an object can be obtained by intersecting the cones defined by the silhouettes of the object in the acquired images and the corresponding viewpoints. Using the inexpensive setup of Figure 1 it is possible to acquire a set of images as the object rotates on a turn table. Assuming a fully calibrated system and an unsupervised procedure for obtaining the silhouettes from the images, a 3D model can be automatically recovered.

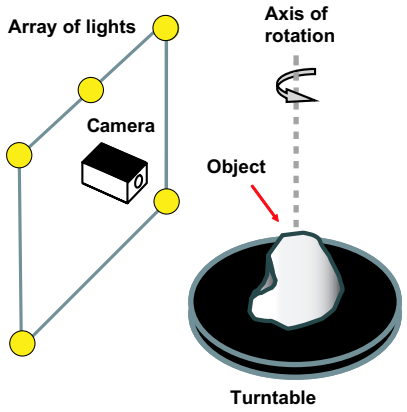

Figure 1: Setup of the shadow carving system.

Shape from silhouette often produces a visually good reconstruction, but this technique fails to model concavities of the object [5]. For this reason different methods have been proposed to improve the estimate obtained from shape from silhouette. These techniques use different visual cues such as color coherence between images (as proposed by Kutulakos and Seitz [6]), or self-shadows (as in Savarese et al. [7]). In particular Savarese et al. proposed to extend the setup of Figure 1 by adding several light sources.

The basic idea is that of comparing the observed shadows to those expected as if the conservative estimate were correct. The current shape is then adjusted to resolve contradictions between the captured images and the current shape estimate. In this process, the volume from the current object estimate is incrementally removed in a conservative way, and in turn, the inconsistencies are reduced. Thus, a closer object's shape estimate is computed at each step. This procedure is called *shadow carving*.

Proceedings of the Third International Symposium on
3D Data Processing, Visualization, and Transmission (3DPVT'06)
0-7695-2825-2/06 $20.00 © 2006 IEEE

We extend the shadow carving idea by considering not only contradictions between observed and simulated shadows, but also contradictions between lit areas of the object and the simulated lit areas of the object estimate. When a lit portion of the object is observed in an image we test whether the corresponding region of the object estimate is also lit. To test this we simulate the process of lighting by using a *Ray Tracing algorithm*. If a contradiction is detected we update the estimate to resolve it. We call this technique *inverse ray-tracing carving (IRT-carving)* because it uses the same principle of ray-tracing algorithms to obtain a 3D object from 2D images. This is in opposition to the common ray-tracing case where an image is obtained from a known 3D scene.

Our analysis shows that IRT-carving can indeed improve the estimation of the object obtained by shadow carving only. This is the main result of this paper. We show that shadow carving do not take full advantage of the available information. That is, given the same available information (number of views and number of lights), IRT-carving allows carving additional pieces of volume and, thus further refining the object estimate.

A second key result is that we prove that IRT-carving is always conservative, i.e. it never removes parts of the acquired object. This is an important property in that it guarantees that the carving process always converges to an upper bound estimate of the object surface.

The remainder of this paper is organized as follows. After a review of previous works in Section 2, we describe our technique in Section 3. We present an analysis of our solution in Section 4, we describe a possible implementation of our technique and show preliminary experimental results with synthetic objects in Section 5. We draw the conclusions in Section 6.

2 Background

The idea of using shadows for shape recovery has a long history. Many researchers studied the constraints based on the observation of shadows and self-shadows and developed methods that enable inference about object shape based on those cues. Pioneering work was presented by Shafer and Kanade [8] and Hambrick et al. [9]. Since then, several methods for estimating shape from shadows have been presented. Kriegman and Belhumeur [10] showed that for any finite set of point light sources illuminating an object there exists an equivalence class of object shapes having the same set of shadows. They used this analysis to infer information about the object shape. Hatzitheodorou and Kender [11] presented a method for computing a surface contour formed by a slice through an object illuminated by a directional light source casting sharp shadows. Raviv et al. [12] developed an extended shape from shadows method based on the idea of *shadowgram*. Similar to Hatzitheodorou and Kender, by identifying beginning and ending shadow points for each light position, the height difference between the points can be computed. Langer et al. [13] extended the method of Raviv et al. for computing holes beneath the recovered height field description of the top surface for 2 dimensions. Daum and Dudek [14] subsequently developed a method for recovering the surface for light trajectories that are not a single arc. Finally, Yu and Chang [15] gave a new graph-based representation for shadow constraints.

All of these methods rely on the accurate detection of the boundaries of shadow regions and are limited to certain object topologies such as 2D-terrains (i.e. bas-reliefs). The work presented by Savarese et al. [7] tried to overcome these limitations by embedding the problem of shape from shadows in multiple view framework.

Our work extends and complements *shadow carving* [7] in that we propose to exploit an additional constraint. Rather than comparing shadow regions for consistency, we check that the lit areas measured on the real object surface do not *appear* as shadows on the current estimate of the object. Likewise *shadow carving*, our method does not require any restriction to 2.5D terrains, rather it allows an in round reconstruction of the object.

Our proposed approach is similar in gist to the space carving approach of Kutulakos and Seitz [6] and to the extensive literature that followed that idea. Our approach differs from [6] in that we consider consistency between a camera and light views, rather than multiple camera views [16].

3. Proposed solution

To simplify the discussion we introduce the *epipolar slice model* presented in [7]. Consider the setup of Figure 2a with a 3D shape, a camera C and a single light source L: the camera center C and the light L define a family of planes P_L that sweeps the 3D space. For each member p_L of this family we obtain an epipolar slice of the space, and in each slice we have an image line l_i, and a 2D region $\mathcal{R}$ obtained by the intersection of the plane p_L with the 3D shape, as shown in Figure 2b. Because the family of epipolar planes P_L sweeps the shape volume, results shown in the following sections can be immediately extended to the 3D case.

In shadow carving [7], a conservative estimate of the shape of an object is progressively carved in order to eliminate every detected contradiction between the shadows the object cast on itself and the ones that the estimate should cast on itself. Consider the simple example of Figure 3a: a camera C is facing an object with a concavity, and a conservative estimate is available. The existence of the concavity in the real object is indicated by the two shadows cast by the two light sources L_1 and L_2; these shadows are

Proceedings of the Third International Symposium on
3D Data Processing, Visualization, and Transmission (3DPVT'06)
0-7695-2825-2/06 $20.00 © 2006 IEEE

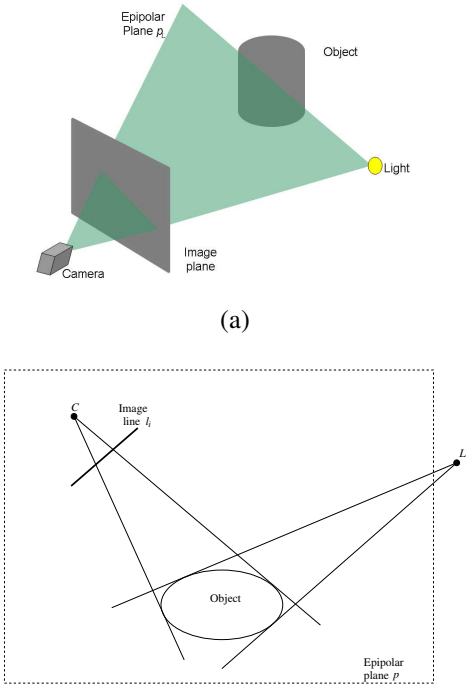

Figure 2: The epipolar slice model.

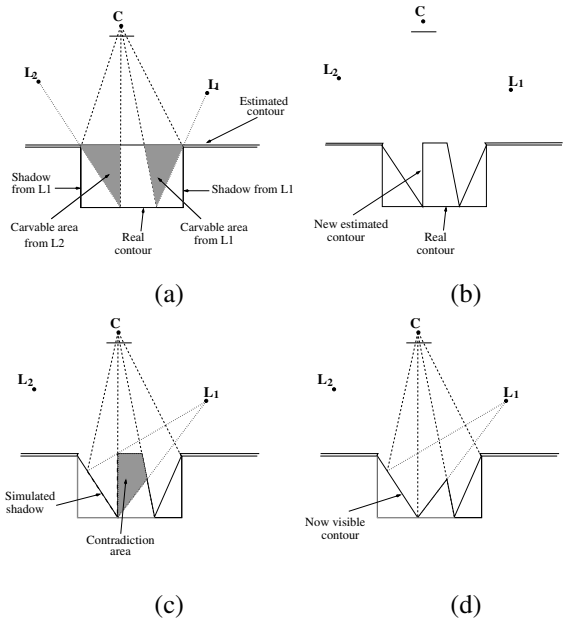

Figure 3: (a) An incoherent situation for the shadow carving algorithm. (b) The shadow carving estimate. (c) The portion of the estimate which is in contradiction with the part of contour lit by L_1. (d) A new estimate which is coherent with the lit information.

clearly not compatible with the conservative estimate of the object. Shadow carving takes advantage of these incompatibilities to remove portions of the current estimate (i.e., the two shaded areas). After removing the two carvable areas, a new conservative estimate of the object is obtained which is compatible with the shadows observed by the camera. Thus no additional volume needs to be removed according the shadow carving algorithm.

The idea behind IRT-carving relies on the following additional observation: the new conservative estimate may be no longer compatible with the observed *lit* regions of the real object. For example, the light source L_2 would cast a "simulated" shadow on the estimated contour which is not detected by the camera (see Figure 3c). Thus, by considering this additional inconsistency it is possible to remove a new portion of the object estimate as shown in Figure 3c. The new estimate better approximates the real object and it is still conservative, i.e. it still fully contains the acquired object (Figure 3d).

To test the contradiction (i.e., the incompatibility between the real lit contours and the simulated ones) we may simulate the lighting process by using a *Ray-tracing algorithm*.

In the next section we study (analytically) under which conditions it is actually possible to carve the estimated object to resolve inconsistencies.

4. Theoretical analysis

In this section we present a theoretical analysis of the IRT-carving technique. We present sufficient conditions under which the technique returns a new conservative estimate of the object.

In the following discussion we will use the epipolar slice model. Also, we will assume that the real object regions $\mathcal{R}$ and the estimate region $\hat{\mathcal{R}}$ are compact subsets (not necessary connected) of the epipolar slice plane p_L. The frontiers of $\mathcal{R}$ and $\hat{\mathcal{R}}$ are the real and estimated contour, respectively. From the conservative assumption we have that the real contour is always inside $\hat{\mathcal{R}}$. We will also assume that the real contour is "smooth": it can be described by a set of C^1 curves on the epipolar plane.

4.1. Basic definitions

Before presenting our main result we define some basic concepts and quantities used through the following analysis. First we define the property of a contour point p being visible from the camera center C and being lit by the light source L.

Definition 4.1 *A point p on the contour of the region $\mathcal{A}$ is visible from the camera center C if there exists an open segment of the line from C to p that never intersects the given $\mathcal{A}$. If a point p is not visible from C we say it is occluded.*

Proceedings of the Third International Symposium on
3D Data Processing, Visualization, and Transmission (3DPVT'06)
0-7695-2825-2/06 $20.00 © 2006 IEEE

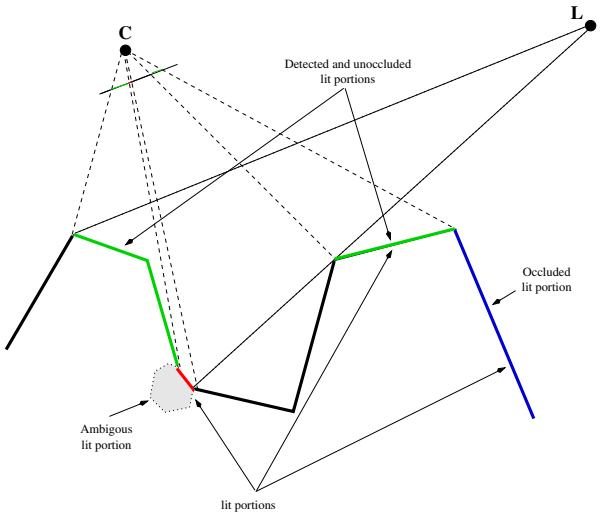

Figure 4: Example of lit contour.

Similarly, a point p on the contour of the region $\mathcal{A}$ is lit by L if there exists an open segment of the line from L to p that never intersects the given $\mathcal{A}$; if a point p is not lit by L we say it is in shadow.

The previous definition depends only on the geometric configuration of the scene: the shape and position of the acquired object, the view point and the light source. Let's assume that a procedure is available that labels points on the image line as lit or as in shadow.

Definition 4.2 *A detected lit point is an unoccluded lit point of the real contour whose projection on the image line l_i is identified as lit by the labeling procedure.*

We will always assume that the labeling procedure is *conservative*, i.e. it never labels as lit the projection of a point p of the real contour that is in the shadow. Figure 4 shows an example of the previous definitions. The colored parts of the contour are the one lit by L, while the black portion are not visible by the light source (shadows). The green portion of the contour are both unoccluded, i.e. visible by the camera C and detectable by the labeling procedure. The blue portion are not visible by the camera C and the red part shows an ambiguous situation for the labeling algorithm. In this case the labeling procedure labels this portion as not lit.

Definition 4.3 *A* simulated *shadow point is a point of the* estimated *contour which is not lit by the light source.*

We emphasize the use of the adjective *simulated* because these points are identified using a ray-tracing algorithm, which is a simulation of the light propagation process. Besides, since we use ray-tracing to cast the rays of light from L we can perfectly detect the simulated shadow points.

If we consider the line that connect an unoccluded lit point on the real contour to the camera source than it must intersect the estimated contour at least in one point, because of the conservative estimate hypothesis.

Definition 4.4 *The closest point to the camera among the intersections of the line defined by the camera center and an unoccluded lit point p is a the reprojected lit point.*

We remark that the lit point p belongs to the real contour while the reprojected lit point belongs to the estimated contour, therefore a property of the real contour is used to characterize the points of the estimated contour.

Definition 4.5 *A point of the estimated contour that is both an unoccluded simulated shadow point and is a reprojected lit one is said to be incoherent. A maximal connected set of incoherent points is named an incoherent region of the estimated contour.*

Definition 4.6 *The union of all the segments that connect the light source L to the points of an incoherent region is said the incoherent cone. The symmetric version of the incoherent cone is said twin cone.*

Definition 4.7 *The intersection between the incoherent cone and the estimate of the real object is the area of interest (AOI).*

Definition 4.8 *The union of the segments that connect all the points in the AOI to the camera center C define the visibility cone. The boundary line of the cone that is closer to light source L is named b_1, while the boundary line that is further from L is named b_2.*

Figure 5 provides an example of the last definitions.

4.2. Conservative carving

After defining all the necessary concepts we can now state the fundamental result of our analysis:

Proposition 4.1 *If the projections of the contour points inside the visibility cone are labeled as lit by the labeling procedure, if the camera center C is inside neither the incoherent nor the twin cone, and if the estimated contour does not cross the line b_2 then it possible to remove the AOI without removing any point of the real object (conservative carving).*

In order to prove Proposition 4.1 we first introduce a notion of partial ordering of the points in the epipolar plane and then prove the following three lemmas.

Definition 4.9 *Given a point p, and assuming that the camera center C does not belong to the line l passing through the light source L and p, we say that a point q is* above *the point p if q is in the half-plane defined by the line l and the camera C.*

Proceedings of the Third International Symposium on
3D Data Processing, Visualization, and Transmission (3DPVT'06)
0-7695-2825-2/06 $20.00 © 2006 IEEE

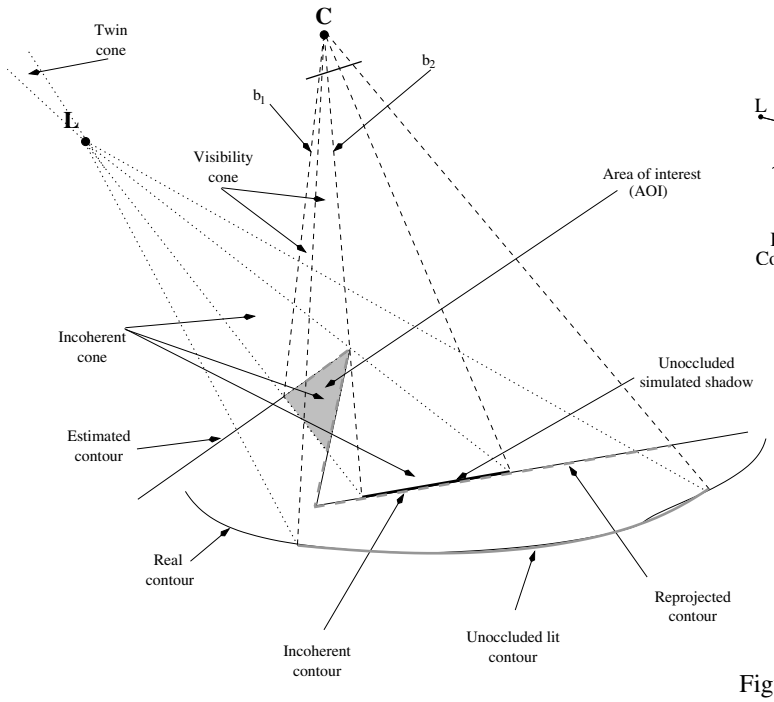

Figure 5: An example of area of interest (AOI) and visibility cone with the two boundary lines b_1 and b_2.

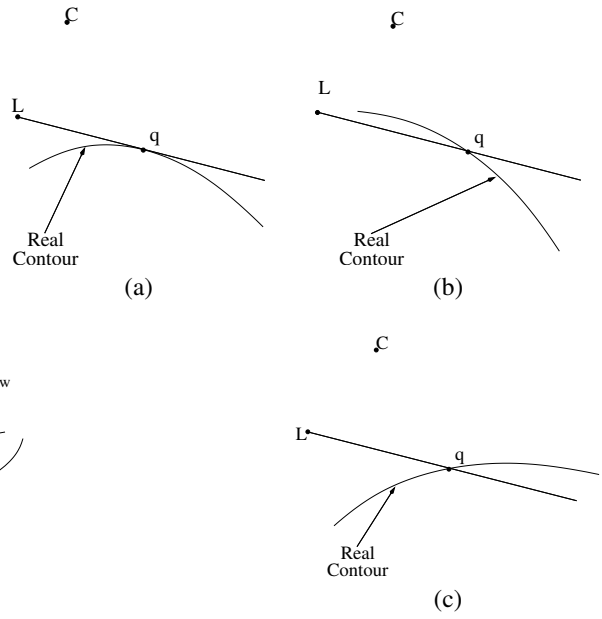

Figure 6: Three possible cases for the point q: (a) tangency, (b) the contour is first above and then below q. (c) the contour is first below and then above q. The case (b) can happen only when q is on the line b_1, and the case (c) can happen only when q is on the line b_2.

Lemma 4.1 *If there is a point p of the real object inside the AOI then there exists a point q inside the visibility cone such that there are no other points of the object inside the visibility that are above the point q. The point q also belongs to the real contour.*

Proof. In the following demonstration we will consider only points of the object that are inside the visibility cone; therefore we will omit this specification.
If there are no points of the object above p then we can set $q = p$ and the conclusion follows. If there is at least another point of the object above p let l be the line passing through the p and the light source L. Consider the not empty set of all the points of the object above p. For each of these we construct a new line through L. Among this set of lines we select the one that creates the greatest angle with l. To find the point q it is now sufficient to chose a point that corresponds to the selected line. The existence of such line and the relative point is due to the hypothesis of compactness of the object slice.
To complete the proof we have to show that q belongs to the real contour. If by contradiction q is an inner point of the object then there exists a small circle that is centered in q and fully contained in the object. Part of the points of the circle are above the point q which contradicts the result of the first part of the lemma. □

Because the point q of Lemma 4.1 is inside the visibility cone, there are only three possible cases: q is strictly inside the visibility cone, q belongs to the boundary line b_1, q belongs to the other boundary line b_2. The following lemma characterizes the relation between the real contour around q and the line l defined by the point q and the light source L.

Lemma 4.2 *If the point q is strictly inside the visibility cone then the line l defined by the light source L and the point q is tangent to the real contour in q as shown in Figure 6a. If the point q belongs to the line b_1 then either l is tangent to the contour in q or it crosses the contour as shown in Figure 6b. If the point q belongs to the line b_2 then either l is tangent to the contour in q or it crosses the contour as shown in Figure 6c.*

Proof. Let us consider the first case, i.e. the point q is inside the visibility cone. Assuming by contradiction that the line l is not tangent to the real contour in q, then the real contour must cross the line l in q, as depicted in Figure 6b or Figure 6c. Because the point q is strictly inside the visibility cone then a finite portion of the real contour passing through q must be also strictly inside the visibility cone. Therefore there must be another point of the real shape that is both inside the visibility cone and *above* q, in contradiction to Lemma 4.1.

Proceedings of the Third International Symposium on
3D Data Processing, Visualization, and Transmission (3DPVT'06)
0-7695-2825-2/06 $20.00 © 2006 IEEE

Let us consider the first case. Assuming by contradiction that the case presented in Figure 6c holds, then because the point q lies on b_1 then there in another point inside the visibility cone above q, which again contradicts Lemma 4.1. Consider the last case, i.e. q belongs to the line b_2. Assuming by contradiction that the case of Figure 6b, then again we have a portion of the contour above the line and inside the visibility point, which contradicts the Lemma 4.1. □

From Figure 6 we conclude that in both the first case and the second one a portion of the contour is occluded from the light source and is strictly inside the visibility cone.

Lemma 4.3 *If there is a point p of the real object in the AOI, if the camera center C is inside neither the incoherent cone nor the twin cone, and if the estimated contour does not cross the line b_2 inside the visibility cone then there is a finite portion of the real contour which is not lit by the light source and is visible by the camera.*

Proof. From the existence of p and from Lemma 4.1 there exists a second point q that belongs to the real contour as well as to the visibility cone and that does not have any other point of the object above itself and inside the visibility cone. Because the estimated contour does not cross the line b_2 inside the visibility cone then the real contour does not cross the line b_2 either. As a result the point q is either on the line b_1 or strictly inside the visibility cone. From Lemma 4.2 there are only two possibilities: (1) the point is a tangent point for the line l defined by L and q, (2) the point is not a tangent point for the line l (and therefore q belongs to the line b_1). In the first case either q is an isolated tangent point (as shown in Figure 6a) or all the points in a neighborhood of the contour are tangent points, i.e. the contour is locally a straight line (flat contour). In both circumstances by the hypothesis on the position of the camera C and because q does not have any points above itself, a finite portion of the contour that is not lit by L is also visible from the camera[1]. In the second case the situation of Figure 6b holds; therefore there is a portion of the real contour not lit by the light source L. By the hypothesis on the position of the camera C and because q does not have any points above itself, a finite portion of the contour that is not lit by L is also visible from C. □

Using the results of the three previous lemmas we can now prove Proposition 4.1.

Proof. If by contradiction there is a point of the object in the AOI then from Lemma 4.3 a not lit portion of the contour is visible from the camera C. Because the labeling procedure is always conservative it must label as shadow the projection of this portion of the contour. Therefore we have a contradiction. □

[1] In the case of flat contour we assume that the region of tangent points is detected as not lit by our labeling procedure.

4.3. Discussion

The main idea of the previous analysis is that if there is a point of the object in the AOI, then there will be also a portion of the real contour inside the visibility cone that is not lit by L and visible from C: therefore, if the projection of the visibility cone on the image plane is labeled as lit, we can safely carve the AOI from the actual estimate. However if the point q belongs to the line b_2 then the not lit portion of the contour related to q can be outside the visibility cone. At that end we have introduced in Prop 4.1 we introduce the hypothesis that the estimated contour (hence the real contour) does not cross the line b_2 inside the visibility cone. This hypothesis can be tested using the available information: the estimated contour, the light source position and the camera center.

The hypothesis on the position of the camera center C is necessary to have the not lit contour visible from camera. This hypothesis is easily met by our acquisition setup.

Finally, we observe that for a given incoherent cone there can be multiple AOI's and visibility cones. If that is the case, it is necessary to verify that Prop 4.1 holds for all the visibility cones before removing the corresponding AOI's.

5. Implementation and experimental results

Based on the result of Proposition 4.1, we can implement an algorithm that can safely remove the portions of the estimated shape that are not coherent with the detected lit surfaces.

Starting from a point on a lit region of the estimated contour, we move toward the light source L with a suitable step size. If we never cross the surface then there is no incoherence and it is not necessary to carve the object. If we intersect the estimated surface, let's call the intersection point r. Then, we need to check for other intersections of the estimated object with the line defined by r and the camera center C. After crossing the estimated contour we keep on moving toward L and at each step we check if the projection of the current point is labeled as lit or not. If for all the steps inside the estimated contour the reprojection is labeled as lit, then we can safely remove the AOI.

Our implementation uses voxels [6] to represent the object estimate and to identify the portion to carve. However different implementations that do not discretize the volume of the object estimate are also possible. A Marching cube algorithm is used to extract a surface from the voxel representation. The extracted surface is then processed using Taubin filtering algorithm [17] to remove fine scale artifacts.

Proceedings of the Third International Symposium on
3D Data Processing, Visualization, and Transmission (3DPVT'06)
0-7695-2825-2/06 $20.00 © 2006 IEEE

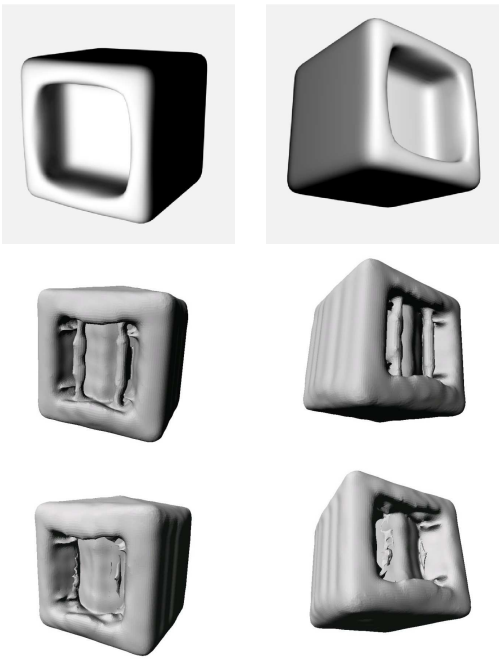

Figure 7: First row: two views of the synthetic object used in the experiment. Middle row: two views of the reconstruction using only shadow carving. Last row: two views of the reconstruction using shadow carving and IRTcarve.

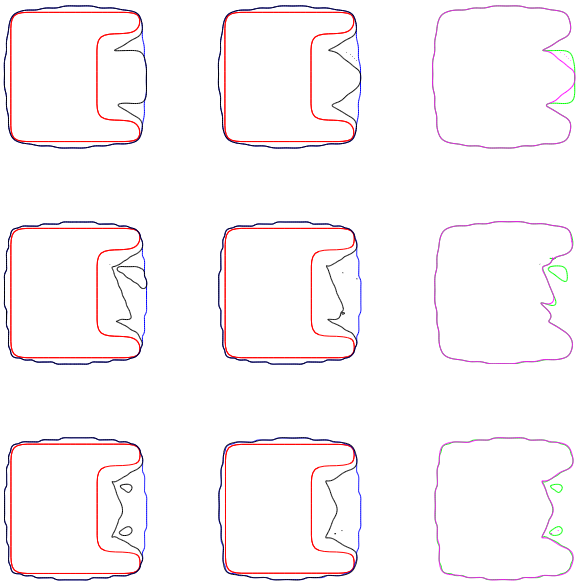

Figure 8: Comparison between the shadow carving algorithm (first column), and the IRT-carving algorithm (second column). The last column compare directly the two estimated contour (green for shadow carving and magenta for the IRT-carving). The first row shows result of the carving from the first viewpoint (0 degree), the second shows 4 viewpoints (90 degrees of rotation), and the last row present result for all 12 viewpoints.

5.1. Experiments with a synthetic object

To evaluate the performance of the algorithm as well as the correctness of our implementation we simulate the acquisition of some simple objects using a 3D modeling software. The advantage of this procedure is to have a controlled setting with a ground-truth for the object we want to reconstruct, as well as a correct labeling procedure. The object used in the simulated experiment is presented in Figure 7 first row, while the acquisition setup is very similar to the one proposed in [7] (see Figure 1).

Because we do not know which sequence of carving leads to the best estimate of the acquired object we adopt the following criteria for the carving sequence: for each position of the camera we first run the shadow carving using all the light sources for that position (in a fixed arbitrary order); the resulting new estimate is then processed by the IRT-carving in order to remove the portions of the volume that are not coherent with the lit parts of the real surface detected in the images.

Figure 7 shows a comparison between the shadow carving algorithm and the combination of shadow carving and IRT-carving algorithm: the central row shows two views of the reconstruction from shadow carving only; the last row shows two views of the reconstruction of shadow carving and IRT carving combined.

Figure 8 shows a comparison between the sections of the two reconstructions. The left column shows cross sections of the real object (red) the initial estimate (blue) and the shadow carving estimate (black) for different camera positions. In the central column the black contour is a cross section of the result of both shadow carving and IRT-carving. Finally, on the right we see the comparison between the shadow carving estimate (green) and the IRT-carving estimate (magenta).

The sections in the first row are obtained using only one viewpoint, and two lights: in this case the IRT-carving yields a better estimate than shadow carving.

As we increase the number of viewpoints, we notice two effects: i) ITR- carving is still improving over the shadow carving estimate; ii) the intermediate shadow carving estimate is more accurate since the starting object volume is a closer approximation of the real one. Overall these two effects lead to a final better estimate of the real object. In particular the two artifacts created by shadow carving in the concavity of the object are removed.

Proceedings of the Third International Symposium on
3D Data Processing, Visualization, and Transmission (3DPVT'06)
0-7695-2825-2/06 $20.00 © 2006 IEEE

6. Conclusions and future work

We have presented a new technique, the *inverse ray-tracing carving (IRT-carving)*, for refining an upper bound estimate of the shape of an object. This technique finds inconsistencies between the lit portions of the object detected in the acquired images, and the simulated lit portions and shadows obtained by means of ray-tracing. It then updates the estimate in order to remove such inconsistencies.

IRT-carving is complementary to shadow carving. On a system level, the volume reconstructed by shadow carving may be used as the input to IRT-carving. Our analysis has shown that IRT-carving can indeed improve the estimation of the object obtained by shadow carving given the same available information (i.e., number of views and number of lights).

The conditions for a conservative carving have been found and studied analytically. The proposed reconstruction technique requires that the acquisition setup is fully calibrated and that the object surface is smooth. Similar assumptions hold for shadow carving. Finally, we have presented preliminary experiments on a synthetic object that validate our theoretical study.

As an extension to this work, it would be interesting to characterize the bound on the precision that can be resolved in this context and address questions such as: Which shape can be recovered exactly? Which ones are ambiguous? Should we use lit and/or shadowed regions? What is the influence of the unclassified areas?

References

[1] J.-Y. Bouguet and P. Perona, "3d photography on your desk," in *Proc. 6th Int. Conf. Computer Vision*, 1998.

[2] W. N. Martin and J. K. Aggarwal, "Volumetric descriptions of objects from multiple views," *IEEE Transactions on Pattern Analysis and Machine Intelligence*, vol. 5, no. 2, pp. 150–158, Mar. 1983.

[3] B. Leibe, Thad Starner, William Ribarsky, Zachary Wartell, David M. Krum, Justin Weeks, Brad Singletary, and Larry F. Hodges, "Toward spontaneous interaction with the perceptive workbench," *IEEE Computer Graphics & Applications*, vol. 20, no. 6, pp. 54–65, Nov. 2000.

[4] R. Szeliski, "Rapid octree construction from image sequences," *Computer Vision, Graphics and Image Processing*, vol. 58, no. 1, pp. 23–32, July 1993.

[5] A. Laurentini, "How far 3D shapes can be understood from 2D silhouettes," *IEEE Transactions on Pattern Analysis and Machine Intelligence*, vol. 17, no. 2, pp. 188–195, Feb. 1995.

[6] K. N. Kutulakos and S. M. Seitz, "A theory of shape by space carving," in *Proc. of the Seventh IEEE Interational Conference on Computer Vision*, Kerkyra, Greece, Sept. 1999, pp. 307–313.

[7] S. Savarese, H. Rushmeier, F. Bernardini, and P. Perona, "Shadow carving," *Proc. of the Int. Conf. on Computer Vision*, 2001.

[8] S. A. Shafer and T. Kanade, "Using shadows in finding surface orientations," *Computer Vision, Graphics and Image Processing*, vol. 22, pp. 145–176, 1983.

[9] L. N. Hambrick, M. H. Loew, and R. L. Carroll, "The entry-exit method of shadow boundary segmentation," *IEEE Transactions on Pattern Analysis and Machine Intelligence*, vol. 9, no. 5, pp. 597–607, Sept. 1987.

[10] D. Kriegman and P. Belhumeur, "What shadows reveal about object structure," *Journal of the Optical Society of America - A*, vol. 18, no. 8, 2001.

[11] M. Hatzitheodour and M. Kender, "An optimal algorithm for the derivation of shape from shadows," in *Proc. of Computer Society Conference on Computer Vision and Pattern Recognition*, Ann Arbor, MI, June 1988, pp. 486–491.

[12] D. Raviv, Y.-H. Pao, and K. A. Loparo, "Reconstruction of three-dimensional surfaces from two-dimensional binary images," *IEEE Transactions on Robotics and Automation*, vol. 5, no. 5, pp. 701–710, Oct. 1989.

[13] M. S. Langer, G. Dudek, and S. W. Zucker, "Space occupancy using multiple shadow images," in *Proc. of the International Conference on Intelligent Robotics and Systems*, Pittsburg, PA, August 1995.

[14] M. Daum and G. Dudek, "On 3-D surface reconstruction using shape from shadows," in *Proc. of Computer Society Conference on Computer Vision and Pattern Recognition*, Santa Barbara, CA, June 1998, pp. 461–468.

[15] Y. Yu and J. Chang, "Shadow graphs and 3D texture reconstruction," *International Journal of Computer Vision*, vol. 62, no. 1-2, pp. 35–60, 2005.

[16] Camillo J. Taylor, "Surface reconstruction from feature based stereo.," in *ICCV*. 2003, pp. 184–190, IEEE Computer Society.

[17] G. Taubin, "A signal processing approach to fair surface design," in *SIGGRAPH*, 1995.

Proceedings of the Third International Symposium on
3D Data Processing, Visualization, and Transmission (3DPVT'06)
0-7695-2825-2/06 $20.00 © 2006 IEEE